

boudin is required for septate junction organisation in *Drosophila* and codes for a diffusible protein of the Ly6 superfamily

Assia Hijazi, Wilfried Masson, Benoit Augé, Lucas Waltzer, Marc Haenlin and Fernando Roch*

The Ly6 superfamily, present in most metazoan genomes, codes for different cell-surface proteins and secreted ligands containing an extracellular motif called a Ly6 domain or three-finger domain. We report the identification of 36 novel genes coding for proteins of this family in *Drosophila*. One of these fly Ly6 proteins, coded by the gene *boudin* (*bou*), is essential for tracheal morphogenesis in the fly embryo and contributes to the maintenance of the paracellular barrier and the organisation of the septate junctions in this tissue. Bou, a glycosylphosphatidylinositol anchored membrane protein, is also required for septate junction organisation in epithelial tissues and in the chordotonal organ glial cells, but not in the central nervous system. Our study reveals interesting parallels between the Ly6 proteins of flies and vertebrates, such as the CD59 antigen. Similarly to this human protein, Bou travels from cell to cell associated with extracellular particles and, consistently, we show that it is required in a non-cell-autonomous fashion. Our work opens the way for future studies addressing the function of Ly6 proteins using *Drosophila* as a model system.

KEY WORDS: Ly6/uPAR, Three-finger toxin, Septate junctions, Paracellular barrier, Blood-brain barrier, Tracheal morphogenesis, *Drosophila*

INTRODUCTION

Model organisms, such as the fruit fly, are sophisticated tools that have contributed decisively to our understanding of genetic complexity, allowing functional characterisation of new genes and novel insight into many developmental processes. We have profited from the advantages offered by *Drosophila* to enlarge current knowledge about a poorly characterised family of proteins present in metazoan genomes, the Ly6 superfamily. The Ly6 proteins share an extracellular motif spanning about 100 residues known as a three-finger domain, three-finger snake toxin motif or Ly6/uPAR domain. This structure, first identified in the sea-snake erabutoxin b (Low et al., 1976), features a simple inner core stabilised by disulphide bridges, which supports three protruding loops or fingers. Besides a diagnostic set of 8 or 10 cysteines found in stereotyped positions, Ly6 primary sequences are poorly conserved, but they adopt remarkably similar three-dimensional structures (Kini, 2002; Ploug and Ellis, 1994). The Ly6 module is a structural domain involved in protein-protein interactions, tolerating an unusual degree of variation and binding with high specificity to a broad spectrum of targets.

The human genome codes for 45 members of the Ly6 superfamily (Galat, 2008). These include 12 TGF β receptors, the ectodomains of which adopt the three-finger fold, but also many glycosylphosphatidylinositol (GPI)-anchored proteins and soluble ligands. Only a few of these proteins have been studied in detail, such as the urokinase plasminogen activator receptor (uPAR; PLAUR – Human Gene Nomenclature Database), which plays important roles

in cell adhesion, proliferation and migration (Blasi and Carmeliet, 2002), and CD59, an inhibitor of complement activity (Davies et al., 1989). Other members, such as Lynx1 (Miwa et al., 2006) or the soluble SLURP proteins (Grando, 2008), act as regulators of nicotinic acetylcholine receptors, and are likely to be the ancestors of the snake neurotoxins. However, although they are often used as lymphocyte and tumoural markers (Bamezai, 2004), many Ly6 human and murine proteins have unknown roles.

We carried out a systematic search for members of the Ly6 superfamily in *Drosophila*, identifying 36 previously uncharacterised genes coding for one or more Ly6 motifs. We also explored the function of one of these proteins during *Drosophila* development, that encoded by the gene *boudin* (*bou*). Phenotypic analysis of *bou* mutants shows that this Ly6 protein participates in the formation of paracellular barriers in epithelial and neural tissues, physiological fences that regulate the passage of solutes between cells in both epithelial and glial sheaths (Banerjee and Bhat, 2007; Tepass et al., 2001). We show that *bou* is required for the organisation of septate junctions (SJs), invertebrate adhesion structures fulfilling an equivalent role to the vertebrate tight junctions. Differing from known SJ constituents, *bou* requirements are non-cell-autonomous, and, accordingly, we find that Bou can be released in extracellular particles and become incorporated into neighbouring cells. Altogether, our results indicate that *Drosophila* could be an attractive system in which to study the function and general properties of Ly6 proteins in a developmental context.

MATERIALS AND METHODS

Sequence analysis

We used the PSI-BLAST algorithm (Altschul et al., 1997) and the Rtv, CD59 and uPAR sequences as queries against the *Drosophila* RefSeq database (Pruitt et al., 2007). Newly identified Ly6 homologues were incorporated into the search matrix until no more members could be identified, typically after six to seven rounds of iterative search. Then, we used these sequences as novel queries. An identical strategy was used in the honeybee.

Université de Toulouse UPS, Centre de Biologie du Développement, CNRS UMR 5547, Bâtiment 4R3, 118 route de Narbonne, F-31062 Toulouse, France.

*Author for correspondence (e-mail: roch@cict.fr)

Genetics

Full definitions of these stocks can be found in FlyBase (<http://flybase.org/>): *bou*^{PG27} (*bouGAL4*), *l(1)6Ea*² (*bou*^{let}), *Dp(1;Y) ci⁺y⁺, rtv¹¹, nrg¹⁴, NrgGFP*, *PdiGFP*⁷⁴⁻¹, *UASApollin-Myc*, *apGAL4*, *btGAL4* *UASActinGFP*, *nulloGAL4*, *enGAL4*, *ptcGAL4*, *dppGAL4*, *tubGAL4*, *hsFLP tubGAL80 FRT19A*; *UASmCD8GFP* and *GAL80^{ts}*. The *FM7c-Actin-lacZ* and *FM7c-KrGAL4UASGFP* balancers were used for genotyping. Temperature shifts at 18°C were done 24 hours before dissection in cultures containing third larval instars of the *bou*^{PG27}/*NrgGFP*; *UASHA-Bou*⁺; *GAL80^{ts}*/⁺ genotype. Mutant clones were induced in 48-hour larvae by 1 hour heat shock at 37°C, in *bou*^{PG27} *FRT19A/hsFLP tubGAL80 FRT19A*; *UASmCD8GFP*⁺; *tubGAL4*/⁺ larvae. A *ywFRT19* chromosome was used as control.

Dye injection

Dye diffusion into trachea and chordotonal organs was analysed injecting with a micromanipulator 10 mg/ml 10 kDa rhodamine dextran (Molecular Probes) into the body cavity of stage 16 (14- to 16-hour) embryos (Lamb et al., 1998). Diffusion into the nerve cord was monitored in 22-hour embryos. Samples were visualised with a Leica SP2 confocal microscope within 20-30 minutes of injection.

Molecular biology

Three independent PCR fragments containing the *bou* transcription unit were amplified from *bou*^{let} genomic DNA, cloned and sequenced. The HA-tag was introduced in frame within the Bou coding region by PCR, using specific oligonucleotides and the RE28342 cDNA (DRGC). The HA-BouΔC was generated substituting Gly128 for a stop codon. Both constructs were sequenced and subcloned into pAc5.1 (Invitrogen) for cell transfection or into pUAST (Brand and Perrimon, 1993) for transgenesis.

Cell culture and biochemistry

Cell culture, transfections and antibody staining were carried out as in Koh et al. (Koh et al., 2008). S2 cells co-transfected with pAcDMoe-GFP (kind gift from F. Payre, CBD, Toulouse, France) and pAcHA-Bou or pAcHA-BouΔC were fixed and stained in either permeabilising (PBS, 0.1% Triton-X100) or non-permeabilising (PBS) conditions. Transfected KcD26 (2 × 10⁶) cells were incubated at 25°C for 1 hour in PBS, with or without 1 unit of phosphatidylinositol-specific phospholipase C (PI-PLC, Sigma). Cell proteins were extracted in 1 × RIPA, whereas the extracellular medium was precipitated with TCA-DOC and resuspended in 50 μl of 1 × loading buffer. For each condition, 20 μg of cell extracts and 25 μl of supernatant were run in an SDS-PAGE gel and blotted with anti-HA.

Immunohistochemistry

Sense riboprobes were generated from clone RE28342 for in situ hybridisation (Waltzer et al., 2003). Embryos and larval tissues were fixed for 20-30 minutes in PBS 4% paraformaldehyde. Blocking, washing and overnight incubation with primary and secondary antibodies were carried out in 0.05% Triton-X100 0.1% BSA. Primary antibodies include mouse anti-β-gal (Promega), rabbit anti-β-gal (Cappel), mouse anti-HA (Covance), rabbit anti-HA (Clontech), rabbit anti-GFP (Torrey), anti-NrxIV (gift of H. Bellen, Baylor College of Medicine, Houston, TX, USA), rat anti-Crb (gift of U. Tepass, University of Toronto, Toronto, Canada), and monoclonals 9E10 anti-Myc, anti-2A12, 4F3 anti-Dlg, DCAD2 anti-DECaD, BP104 anti-Nrg and 7G10 anti-FasIII, all from DSHB. Secondary FITC and TRIT conjugated antibodies and streptavidin come from Molecular Probes. We also used CBP-FITC (NEB). Samples were visualised with a Leica SP2 confocal microscope.

RESULTS

The *Drosophila* genome codes for 41 Ly6 family members

In general, Ly6 domains share little sequence similarity, making their identification by genomic annotation algorithms difficult. For instance, the only known *Drosophila* proteins containing this domain are the five TGFβ receptors (*tkv*, *babo*, *sax*, *put* and *wit*) and the product of the gene *retroactive* (*rtv*) (Moussian et al., 2005). Using the iterative PSI-BLAST program (Altschul et al., 1997), we carried out a systematic search for Ly6 members in the fly genome, screening

for domains of about 100 amino acids containing 10 cysteines, where Cys¹ and Cys² are always separated by two residues and an Asn residue contiguous to the last cysteine (canonical 10C motif). Alignment of the *Drosophila* Ly6 domains revealed the presence of short intervening distances between Cys⁸ and Cys⁹ (0-3 residues) and Cys⁹ and Cys¹⁰ (4-5 residues), confirming that they belong to the Ly6 family (see Fig. S1 in the supplementary material). Thus, besides the five TGFβ receptors, we have identified in flies 72 Ly6 canonical motifs and 14 related domains encoded by 36 different genes not previously ascribed to any known family (Table 1).

Ly6 motifs are never found in combination with other extracellular domains, a principle also valid in *Drosophila*, where a single Ly6 domain is the only module present in 28 proteins. In the other eight cases, multiple Ly6 motifs are found, as in the human uPAR and C4.4A proteins (Galat, 2008). We also identified three different types of Ly6-related domains lacking key features of a canonical domain. The first variant found was the 8C domain (11 motifs found in two proteins), with only eight cysteines. Interestingly, 8C domains are similar to the vertebrate uPAR domain I, which lacks both Cys⁷ and Cys⁸ and also the disulphide bridge formed by these residues. Nonetheless, the uPAR domain I also adopts a three-finger fold (Huai et al., 2006). Another variant is what we call 'atypical 10C' domain (a10C), found only in two proteins. This motif could have arisen by replacement of Cys⁸ by a new Cys placed two residues after the C-terminal Asn (see Fig. S1 in the supplementary material). Finally, we found a group of three contiguous genes coding for long stretches of repeated amino acids (mostly Ser, Thr and charged residues) in the region between Cys⁴ and Cys⁵ (see Fig. S1 in the supplementary material). We termed these long motifs 'disordered 10C' (d10C), as these repeats are predicted to form flexible regions of unstable conformation, called regions of intrinsic disorder (Dyson and Wright, 2002). Hence, it is not clear whether these proteins adopt a three-finger fold.

Vertebrate members of the Ly6 family are synthesised as propeptide precursors entering the endoplasmic reticulum thanks to an N-terminal signal peptide. They have often a second C-terminal hydrophobic peptide placed after their Ly6 domain, permitting the addition of a GPI anchor to an internal sequence of the precursor. In *Drosophila*, all the Ly6 genes code for an N-terminal portion of 25-35 residues and a 20- to 30-residue C-terminal stretch, raising the possibility that all could incorporate a GPI anchor.

We could not establish orthology relationships between *Drosophila* and vertebrate Ly6 proteins due to their low degree of sequence similarity. However, for each *Drosophila melanogaster* protein we identified a putative orthologue in *Drosophila grimshawi*, a distant drosophilid species. We found that the organisation of canonical, 8C, a10C and d10C Ly6 motifs is also conserved in this species, despite 60 mya of separate evolution (Tamura et al., 2004) (Table 1). Therefore, the whole fly Ly6 family was already present in the drosophilid ancestor. We also performed a search for Ly6 members in the honeybee genome, finding only 14 genes coding for this motif. Among these, 12 are orthologues of *Drosophila* genes (sequence identity above 50%). Thus, several gene duplication events followed by rapid divergence occurred in the drosophilid lineage, which nonetheless conserved most of the ancestral Ly6 members. Intriguingly, as is also the case in humans and mice (Galat, 2008), the *Drosophila* genes coding Ly6 proteins are often contiguous in the genome, forming six clusters that group together 24 genes (Table 1).

Existing databases of gene expression patterns allowed us to visualise during embryogenesis the transcript distribution of 21 members of the *Drosophila* Ly6 family (Tomancak et al., 2002). They are expressed in a dynamic and tissue-specific pattern in a

Table 1. The *D. melanogaster* Ly6 genes ordered according to their cytological position, indicating inclusion in a genomic cluster (I-VI) and the number of residues of each protein

<i>Dmel</i> gene name	Length	Cytolocation	<i>Dmel</i> cluster	<i>Dgri</i> orthologue	<i>Amel</i> orthologue	Domain composition	Embryonic expression pattern
CG15773	478	5 B3	–	GH24088	–	4×10C + 1×a10C	NA
CG14430 <i>bou</i>	149	6 E4	–	GH24685	XP_001120415	1×10C	Trachea, fore and hindgut, salivary gland
CG15347	214	7 E11	–	GH12232	–	2×10C	Yolk nuclei, midgut
CG1397 <i>rtv</i>	151	10 A8	–	GH12509	NW_001253268.1	1×10C	Trachea, epidermis, head skeleton, pharynx
CG2813	153	21 E2	–	GH11235	XP_001120323	1×10C	Trachea, fore and hindgut, salivary gland
CG7781	147	29 A5	I	GH10175	XP_001120798	1×10C	No staining
CG14275	148	29 B1	I	GH11591	–	1×10C	Yolk nuclei, fat body
CG14274	136	29 B1	I	GH11592	–	1×10C	NA
CG14273	252	29 B1	I	GH11593	–	1×d10C	NA
CG7778	269	29 B1	I	GH11594	–	1×d10C	Late expression in head epidermis, hindgut, anal pad
CG31901	555	29 B1	I	GH11595	–	1×d10C	NA
CG9568	150	29 F7	II	GH13259	–	1×10C	Midgut, Malpighian tubules, gastric caecum
CG13102	150	29 F7	II	GH13260	–	1×10C	Midgut
CG6583	154	33 D2	III	GH11181	XP_001122840	1×10C	NA
CG17218	151	33 D2	III	GH11641	XP_393726	1×10C	Trachea, fore and hindgut, salivary gland
CG6579	185	33 D2	III	GH10139	–	1×10C	NA
CG15170	561	37 B8	IV	GH11596	–	3×10C + 1×a10C + 2×8C	NA
CG15169	345	37 B8	IV	GH10174	–	1×10C	NA
CG10650	425	37 B8	IV	GH10197	–	5×10C	Midgut
CG31676	159	38 F2	V	GH10589	–	1×10C	Gonad, prothoracic muscle, ring gland
CG9335	166	38 F2	V	GH10590	–	1×10C	Bolwig organ, ventral nerve cord, lateral glia
CG9336	148	38 F3	V	GH10591	–	1×10C	Dorsal vessel, ventral nerve cord, peripheral nervous system
CG9338	147	38 F3	V	GH10592	–	1×10C	Dorsal vessel, peripheral nervous system, trachea
CG31675	148	38 F3	V	GH10593	–	1×10C	Peripheral nervous system
CG14401	146	38 F3	V	GH10594	–	1×10C	NA
CG33472	158	47 F13	–	GH21388	NW_001253216	1×10C	NA
CG8501	152	49 A1	–	GH20694	–	1×10C	NA
CG3955	201	49 F2	–	GH21594	XP_623481	1×10C	NA
CG6329	155	50 C6	–	GH21037	XP_395132	1×10C	Ventral nerve cord
CG13492	2968	58 A2	VI	GH20775	–	27×10C + 7×8C	NA
CG34040	281	58 A2	VI	GH20774	–	2×10C	NA
CG4363	199	58 A2	VI	GH20773	–	2×10C	No staining
CG4377	231	58 A2	VI	GH20772	–	2×10C	NA
CG6038	158	68 D2	–	GH16386	NW_001253250.1	1×10C	Pharynx, hindgut, epidermis
CG8861	180	85 D8	–	GH22350	XP_397506	1×10C	Ventral nerve cord
CG31323	169	97 A2	–	GH19467	XP_001121813	1×10C	Midgut

A. mellifera and *D. grimshawi* accession numbers correspond to annotated proteins or contigs coding for the corresponding orthologues. Domain composition refers to the number of times (1×, 2×, etc.) a domain appears in a protein (10C, canonical domain; a10C, atypical domain; d10C, disordered domain; 8C, 8 cysteines domain; see text for definitions). Expression patterns descriptions are as in Tomancak et al. (Tomancak et al., 2002), except for *CG1397 rtv*, which is described by Moussian et al. (Moussian et al., 2005). NA, not available.

wide range of contexts, from the epidermis and its derivatives to the nervous system and the gut (Table 1). Thus, Ly6 genes can potentially participate in many different developmental and physiological processes.

The *bou* product is required for tracheal morphogenesis

We analysed the function of a new member of this family, the product of the *CG14430* gene, which we have called *boudin* (*bou*). The *bou* locus codes for a protein of 149 residues presenting all the typical features of Ly6 members. Bou is predicted to be a GPI-anchored protein by the Big-PI algorithm (Eisenhaber et al., 1998), which proposes Asn125 as the omega site of the mature protein, where the GPI moiety is attached (Fig. 1B). Unlike other members of the *Drosophila* Ly6 family, the Bou sequence appears conserved in other insect genomes, where we have identified clear orthologues (Fig. 1C).

The *bou* transcript was first detected by in situ hybridisation at the cellular blastoderm stage, first ubiquitously and then accumulating in the invaginating mesoderm (Fig. 1D-F). By stages 13 and 14, the hindgut, foregut, salivary gland and tracheal cells express high levels of *bou*, which is also present at lower levels in the epidermis (Fig. 1G,H). This pattern is maintained until the end of embryogenesis, although transcript levels start declining after stage 14 (Fig. 1I). We did not detect *bou* expression in the ventral nerve cord or in mesodermal derivatives, indicating that at late stages this gene is expressed only in ectodermal tissues.

In a genetic screen we recovered a GAL4 P-element embryonic lethal insertion in the 5' UTR of *bou* (*bou*^{PG27}) (Fig. 1A) (Bourbon et al., 2002). Both remobilisation of this transposon or expression of an HA-tagged Bou form (HA-Bou), using *bou*^{PG27} itself as driver, restored the viability of *bou*^{PG27} flies. We used this allele to carry out complementation tests with lethal mutations mapping to the same

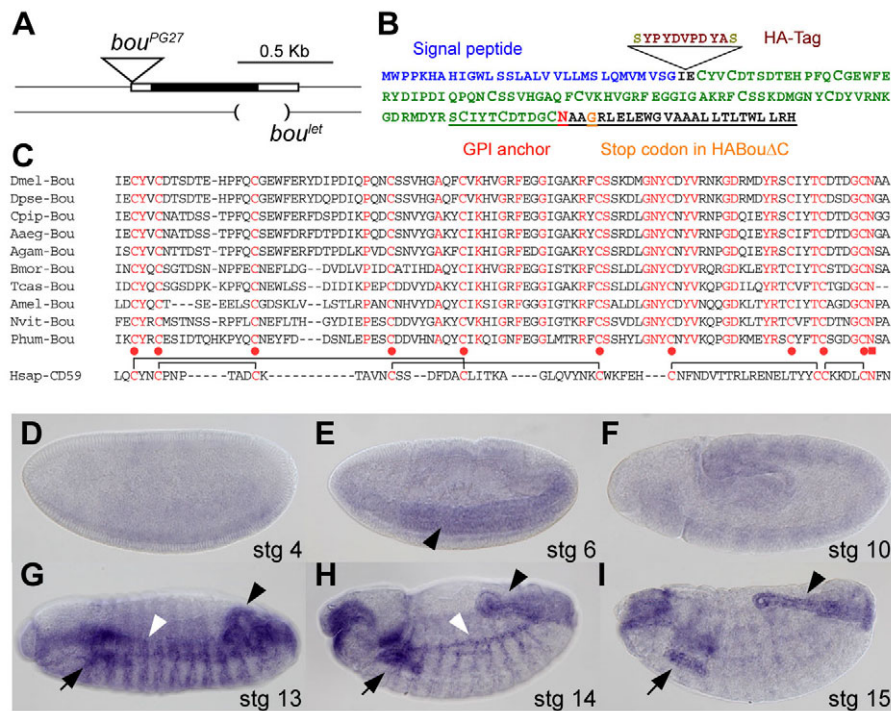


Fig. 1. *bou* codes for a conserved Ly6 protein. (A) The *bou* locus, indicating the *bou*^{PG27} and *bou*^{let} DNA lesions. (B) Bou precursor features: the signal peptide (indigo), the Ly6 domain (green) and the putative GPI anchor site (Asn125, red). The HA-tag position (brown) and the HA-BouΔC stop codon (orange) are also indicated. Residues deleted in the *bou*^{let} mutant are underlined. (C) Protein alignments of the Ly6 domain of insect Bou orthologues and human CD59, showing its stereotyped pattern of disulphide bridges. The 10 conserved Cys and Asn residues are indicated by red dots or a square, respectively. (D-I) *bou* expression during embryogenesis. *bou* mRNA is upregulated in the invaginating mesoderm (E, black arrowhead). At stages 13 and 14 (G-H), it accumulates in the hindgut (black arrowhead), salivary gland (black arrow) and trachea (white arrowhead), before its levels start decaying by stage 15 (I).

chromosomal region and identified a second *bou* lethal mutation, *l(1)6Ea²* (*bou*^{let}) (Perrimon et al., 1989). Sequencing of the *bou* region in the *bou*^{let} chromosome revealed a deletion of 238 nucleotides encompassing the coding region and most of the 3' UTR (Fig. 1A). We predict *bou*^{let} to be a null allele, as this deletion truncates the Ly6 domain and eliminates the C-terminus of the Bou precursor (Fig. 1B).

As *bou* is expressed in the tracheal cells, we first looked for morphological defects in this tissue. Staining with the 2A12 tracheal luminal marker and labelling of tracheal cells with ActinGFP revealed that *bou*^{PG27} and *bou*^{let} embryos display identical phenotypes, presenting tracheal tubes with abnormal shape and dimensions (Fig. 2A-H; and data not shown). At stage 16, the branch pattern of the tracheal network seemed normal, but the dorsal trunk appeared elongated and convoluted and we observed that the 2A12 luminal staining was interrupted along the dorsal branches and transverse connectives (Fig. 2B,E). These phenotypes point to tracheal lumen expansion defects (Beitel and Krasnow, 2000), and indeed, the tracheal dorsal trunk of stage 15 *bou* mutants did not present a uniform width (Fig. 2W), showing instead a series of bulging cysts resembling a string of sausages (hence the name 'boudin', a French black sausage).

The Ly6 genes *bou* and *rtv* regulate tracheal morphogenesis through different mechanisms

The defects observed in *bou* trachea were strikingly similar to those seen in mutant embryos for *rtv*, a gene coding for another Ly6 protein (Moussian et al., 2005). *Rtv* is required for the formation of an intraluminal chitin cable, which is essential for proper tube expansion of *Drosophila* trachea (Devine et al., 2005; Moussian et al., 2006; Tonning et al., 2005). To determine whether *bou* and *rtv* act by similar mechanisms, we monitored chitin cable integrity in stage 16 *bou* mutants, using a fluorescent chitin-binding probe (CBP). Chitin forms an organised filamentous structure in the lumen of wild-type trachea, but in the *rtv*^{ll} null allele this structure is lost and CBP stains a diffuse luminal material (Fig. 2J-L) (Moussian et

al., 2006). The chitin cable of *bou*^{let} mutants also loses its fibrous aspect, although the CBP staining is more intense than in *rtv*^{ll} trachea (Fig. 2K,L). Thus, chitin cable formation is affected in both *bou* and *rtv* mutants, with *bou* presenting a weaker phenotype.

Mutations in different *Drosophila* SJ components also result in embryos with abnormal trachea, presenting the same cysts observed in *rtv* and *bou* mutants (Beitel and Krasnow, 2000; Wu and Beitel, 2004). As SJs are adhesion structures required for the establishment of paracellular barriers regulating molecular diffusion through epithelia, we examined the integrity of this barrier in both *rtv* and *bou* mutants. For this, we injected 10 kDa fluorescent dextran into the body cavity of live embryos and monitored the capacity of this molecule to enter the tracheal lumen (Lamb et al., 1998). At stage 16, both wild-type and *rtv*^{ll} tracheal cells formed an efficient paracellular barrier, preventing dye diffusion into the lumen (Fig. 2M-R). By contrast, dextran was readily detected inside the *bou*^{let} tracheal tubes within 20 minutes of injection and we observed abnormal dye deposits trapped between contiguous cells (Fig. 2N,Q). Thus, the paracellular barrier is disrupted in *bou* mutants, suggesting that this gene is implicated in SJ organisation. To confirm this hypothesis, we examined the subcellular localisation of an SJ component, Fasciclin3 (Fas3), in tracheal cells (Beitel and Krasnow, 2000; Wu and Beitel, 2004). In wild-type and *rtv*^{ll} tracheal cells, this marker accumulates in the most apical part of the lateral membrane, where SJs are present (Fig. 2S,U). By contrast, this apical accumulation was lost in *bou*^{let} embryos and Fas3 appeared uniformly distributed along the lateral membrane (Fig. 2T). Therefore, whereas *bou* is required for SJ maintenance, *rtv* seems dispensable for this process, indicating that these genes regulate tracheal morphogenesis by different mechanisms.

bou is essential for SJ organisation in *Drosophila* epithelia

To further characterise the *bou* phenotypes, we analysed the subcellular localisation of several SJ components, including Discs large 1 (Dlg1), Neurexin IV (Nrx-IV) and the protein-trap fusion

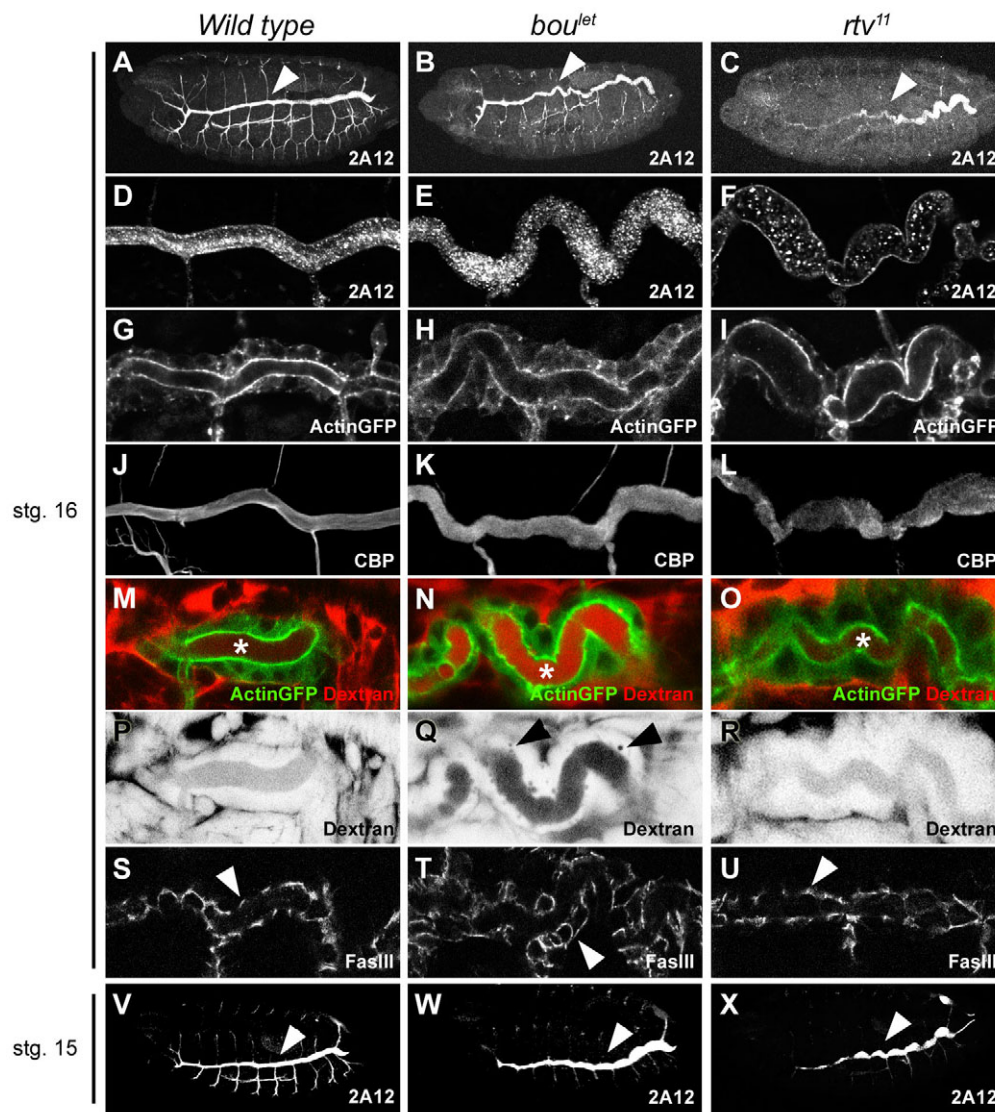


Fig. 2. *bou* and *rtv* regulate tracheal morphogenesis by different mechanisms. Projections (A-C, J-L and V-X) or single confocal sections (D-I and M-U) of embryonic trachea. (A-I) At stage 16, the dorsal trunk of both *bou*^{let} and *rtv*¹¹ mutants displays an enlarged width and a convoluted shape, compared with wild type, as revealed by 2A12 luminal staining (A-F, arrowheads) or cell-contour labelling with ActinGFP (G-I). (J-L) CBP staining reveals luminal chitin cable disorganisation in both *rtv*¹¹ and *bou*^{let} mutants. (M-O) Diffusion of 10 kDa dextran (red) into the trachea (marked by ActinGFP, green) of stage-16 wild-type and mutant live embryos. (P-R) Negative image in black and white of the dextran red channel. Dextran (black) diffuses into the tracheal lumen of *bou*^{let} (N,Q, asterisk) but not wild type or *rtv*¹¹ embryos (M,P,O,R, asterisks). Notice abnormal dye deposits between *bou*^{let} contiguous cells (Q, black arrowheads). (S-U) Fas3 appears delocalised along the lateral membrane of tracheal *bou*^{let} cells (T, arrowhead) but localises to the apical part of both wild-type and *rtv*¹¹ trachea (S,U, arrowheads). (V-X) Stage 15 *bou*^{let} and *rtv*¹¹ embryos stained with 2A12, showing a series of cysts in their dorsal trunk (arrowheads).

NeuroglianGFP (NrgGFP) (Beitel and Krasnow, 2000; Wu and Beitel, 2004). Similarly to Fas3, all these markers appeared delocalised in the lateral membrane of *bou*^{let} tracheal cells (Fig. 3A,G-I,D,J-L). We also monitored the distribution of the cell polarity marker Crumbs (Tepass et al., 1990) and the apical junction component DE-Cadherin (Shotgun – FlyBase) (Oda et al., 1994). As in controls, these markers localised to the most apical part of the tracheal cells throughout development, indicating that *bou* specifically affects the SJ organisation rather than the general polarity of the cell (Fig. 3B,C,E,F). In addition, *bou* is required for the early establishment of SJ in this tissue (see Fig. S2 in the supplementary material), because a clear delocalisation of the NrX-IV marker was already observed by stage 14, when pleated SJ begin to form (Tepass and Hartenstein, 1994).

Finally, we tested if *bou* is required for SJ organisation in other epithelial tissues, such as the epidermis, salivary gland and embryonic hindgut. Analysis of *bou*^{let} embryos showed that NrgGFP, Dlg1 and NrX-IV are also delocalised in these tissues (Fig. 3M-R; and data not shown). Thus, *bou* is generally required for SJ organisation in embryonic ectodermal derivatives.

***bou* is required for SJ formation in a non-cell-autonomous fashion**

Seeking to extend the characterisation of *bou* requirements to larval tissues, we analysed the contribution of this gene to the morphogenesis of imaginal discs, the epithelial precursors of the adult integument. For this, we studied mosaic individuals containing clones of homozygous *bou*^{PG27} cells, using the MARCM technique to positively label the mutant territories (Lee et al., 2000). We found that large *bou* wing clones generated early in larval development did not show any obvious growth defects. Moreover, the SJ marker Fas3 protein was correctly localised in *bou* mutant cells (Fig. 4A-A'). Thus, *bou* function could be restricted to the embryonic tissues or, more intriguingly, the surrounding cells could exert a rescuing activity upon the mutant territories.

To discriminate between these possibilities, we sought to establish whether *bou* is required in larval tissues. To bypass embryonic lethality and recover *bou*^{let} mutant larvae, we expressed wild-type HA-Bou in *bou*^{let} embryos using *nullo*GAL4, a driver only active at the blastoderm stage (Coiffier et al., 2008). In this way, we obtained *bou*^{let} mutants now dying at pupariation and presenting discs with reduced size and abnormal shape. At the

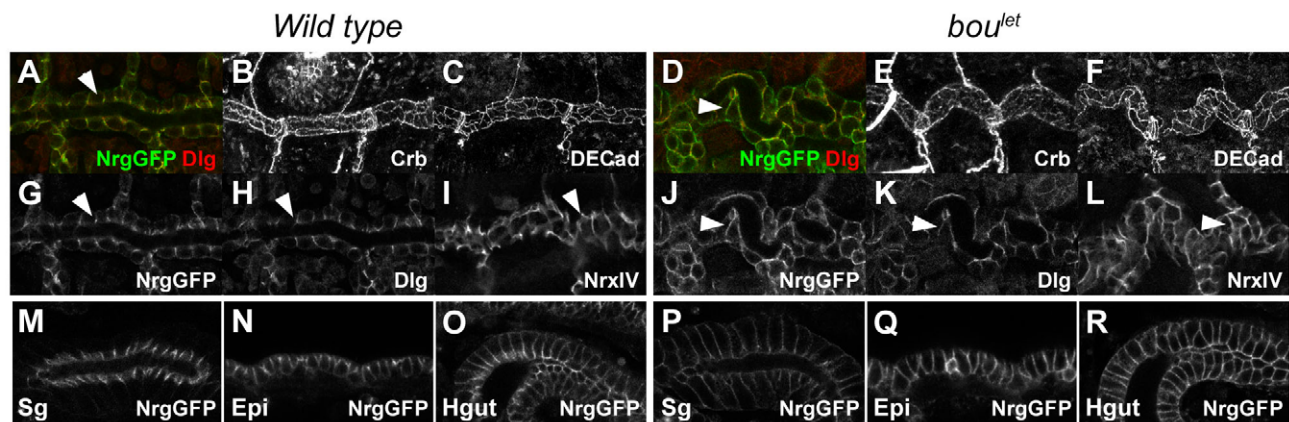


Fig. 3. *bou* is required for septate junction organisation in embryonic ectodermal derivatives. (A-L) Confocal sections of stage-16 tracheal dorsal trunks of wild-type and *bou^{et}* embryos stained as indicated. NrgGFP (G,J, green in A,D), Dlg1 (H,K, red in A,D) and NrX-IV (I,L) distribute along the lateral membrane of *bou^{et}* mutant tracheal cells (D,J-L, arrowheads), differing from the control (A,G-I, arrowheads). The cell markers Crumbs (B,E) and DE-Cadherin (C,F) localise to the most apical part of tracheal cells in both wild-type and *bou^{et}* embryos. (M-R) Confocal sections of stage-16 embryonic salivary glands (M,P), lateral epidermis (N,Q) and hindgut (O,R) labelled with NrgGFP. In the wild type (M-O), these markers localise to the apical part of the cells (towards the lumen in hindgut and salivary glands; up in the epidermis) whereas in the *bou^{et}* mutant (P-R) they spread along the lateral membrane. Epi, epidermis; Hgut, hindgut; Sg, salivary glands.

cellular level, we observed that Crumbs localisation was not affected in *bou^{et}* wing cells. By contrast, the SJ marker Fas3 was delocalised and distributed uniformly along the basolateral membrane (Fig. 4C-F). Thus, the *bou* product is also specifically required for SJ organisation in imaginal epithelia. Consistent with the idea that *bou* phenotypes are not cell-autonomous, we recovered morphologically normal adult *bou^{et}* mutant flies expressing HA-Bou with *engrailed*, *patched* or *decapentaplegic GAL4*, three drivers with clear-cut regionalised patterns. Moreover, staining for Fas3 in *bou^{et}*; *enGAL4/UASHA-bou* mutant discs confirmed that SJs are normal throughout the disc and not only in the *engrailed* domain (Fig. 4B-B'). Therefore, cells expressing the Bou protein can rescue the mutant phenotypes in surrounding territories, confirming that *bou* acts non-autonomously.

One possibility is that Bou itself can travel from cell to cell. Indeed, some vertebrate members of the Ly6 family have the ability to diffuse, either as soluble ligands or coupled to lipid particles via their GPI anchor (Chimienti et al., 2003; Rooney et al., 1993). To gain insight into the Bou mode of function, we generated transgenic flies expressing a C-terminal truncated form of HA-Bou (HA-Bou Δ C), coding for an intact Ly6 motif but missing the last 22 residues of the precursor (Fig. 1B). We predicted this molecule would behave as an active soluble form, as the C-terminal region is necessary for GPI addition in other GPI-anchored proteins. Instead, we observed that HA-Bou Δ C expression did not rescue the *bou^{PG27}* lethality, indicating that the Bou C-terminus integrity is essential for its activity. Moreover, expression of HA-Bou Δ C in the tracheal cells driven by *breathlessGAL4* could not rescue Fas3 delocalisation in *bou^{et}* mutant trachea (Fig. 4J,N,R), whereas expression of a wild-type HA-Bou form not only rescued the *bou^{et}* phenotypes in the tracheal cells but also in the salivary gland and the hindgut, tissues not expressing HA-Bou in this genetic combination (Fig. 4I,M,Q; and data not shown). This finding indicates that Bou-targeted expression can elicit non-autonomous effects in other tissues, opening up the possibility that Bou could diffuse systemically.

Bou localisation is not restricted to SJ membrane areas

To characterise the Bou subcellular distribution, we first sought to confirm whether Bou is a membrane GPI-anchored protein. In *Drosophila* S2 cells, HA-Bou is observed in the cell body and also the plasma membrane, as confirmed by immunostainings carried out in non-permeabilising conditions (Fig. 5A,C). By contrast, the HA-Bou Δ C form could only be detected in internal cell compartments after permeabilisation, showing that the Bou C-terminus is essential for cell membrane insertion (Fig. 5B,D). HA-Bou is a GPI-anchored protein, because incubation of intact cells with phosphatidylinositol phospholipase C (PI-PLC) provokes its release to the extracellular medium (Fig. 5E).

Next, we studied the HA-Bou subcellular localisation in embryonic tissues and in the wing disc, activating its expression with tissue-specific drivers. As in cultured cells, HA-Bou appeared distributed homogeneously throughout the tracheal cell body and did not accumulate in any particular structure (Fig. 6A). We found that the HA-Bou Δ C form has a more restricted localisation, as it was excluded from contact regions between adjacent cells (Fig. 6B). Co-staining with the SJ marker NrgGFP showed that HA-Bou Δ C was absent from the lateral membrane, whereas the HA-Bou staining overlapped with NrgGFP in the apical part of the cells (Fig. 6A,B).

In the wing disc, HA-Bou was also present in the cell body and throughout cell contact regions (Fig. 6C,E,G,H). By contrast, the HA-Bou Δ C form distributed like the disulphide isomerase PdiGFP, a resident enzyme of the endoplasmic reticulum (ER) (Bobinac et al., 2003) (Fig. 6D,F,I,J). Thus, the HA-Bou Δ C form could not exit the ER, whereas the full-size HA-Bou reached membrane areas from which the ER is excluded (Fig. 6C,D,G,I). Co-staining with NrgGFP revealed that HA-Bou was present at the SJ level and accumulated in an apical region, placed above the SJ, that could correspond to a secretion compartment (Fig. 6E,H, see below).

To gain insight into the dynamics of HA-Bou protein localisation, we profited from the large size of the third-larval-instar salivary gland cells. Using the *bou^{PG27}* *GAL4* driver, we drove expression of HA-Bou and HA-Bou Δ C in this cell type, placing a *GAL80^{ts}* thermosensitive repressor in the same genetic background (McGuire

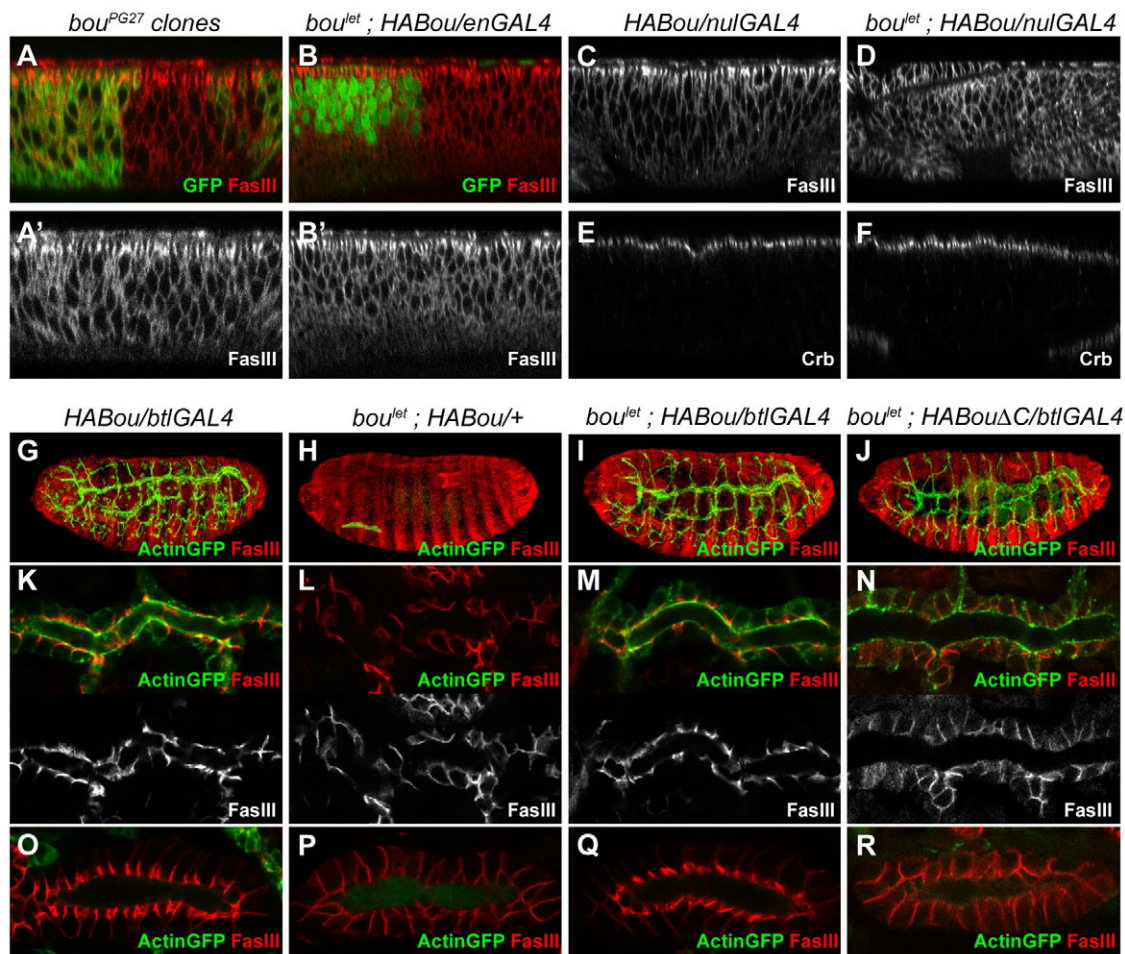


Fig. 4. *bou* SJ phenotypes are not cell-autonomous. (A-F) Confocal z-sections through the pouch of third-larval-instar wing discs. (A,B) Fas3 (red; white in A', B') is correctly localised in all the cells of mosaic wings containing GFP⁺ *bou^{PG27}* mutant clones (A, green) or *bou^{let}* mutants expressing HA-Bou in *enGAL4* GFP⁺ cells (B, green). (C,D) Fas3 distributes along the lateral membrane of *bou^{let}* mutant discs but localises apically in controls. (E,F) Crumbs localises to the apical region of both wild-type and *bou^{let}* mutant wing cells. (G-R) Confocal sections showing Fas3 localisation (red) in wild-type or *bou^{let}* embryos expressing HA-Bou or HA-BouΔC in the tracheal epithelium. Presence of ActinGFP (green) reveals *btlGAL4* driver activity. Only wild-type and HA-Bou-rescued *bou^{let}* embryos display normal accumulation of Fas3 in both trachea (K-N) and salivary glands (O-R). The green extracellular signal seen in salivary glands corresponds to unspecific background staining.

et al., 2003). At 25°C, the GAL80^{ts} repressor is inactive and we observed a strong accumulation of the HA-Bou forms in the salivary gland cell body (Fig. 6K,L). Then, we shifted the larvae at 18°C 24 hours before dissection, activating the GAL80^{ts} repressor and shutting down synthesis of HA-Bou protein. In these conditions, HA-Bou disappeared from the cell body and accumulated at high levels in the lumen of the salivary gland. In addition, we observed a weak but clear staining at the lateral membrane, coinciding with the NrgGFP SJ marker (Fig. 6M). As expected, the levels of HA-BouΔC decayed uniformly after the temperature switch (Fig. 6N). These results confirm that Bou associates with SJ membrane regions, although its localisation is not restricted to these membrane domains.

Bou is secreted extracellularly

One way to explain the non-cell-autonomy of the *bou* phenotypes is that Bou could be secreted extracellularly. Consistently, we noticed the presence of extracellular particles containing this protein in the luminal surface of the wing disc, budding off from the apical HA-

Bou-enriched domain (Fig. 6C; Fig. 7A,B). These particles were seen over *apGAL4*-expressing cells, but were also detected in other territories of the wing disc lumen, indicating that HA-Bou can diffuse (Fig. 7A). Interestingly, increasing the laser power of the confocal microscope, we observed a diffuse intracellular staining and the presence of dots containing HA-Bou in cells adjacent to the *apGAL4* territory, showing that the secreted protein is incorporated by neighbour cells (Fig. 7D). In addition, we observed intracellular vesicles accumulating high levels of HA-Bou within the *apGAL4* cells (Fig. 7C). As none of these structures was observed in HA-BouΔC-expressing discs (Fig. 7E-H), we conclude that they reflect the ongoing traffic of the HA-Bou protein in the wing epithelium. We tested if the Bou extracellular particles are lipophorin particles, as these lipid vesicles are known to contain GPI-anchored proteins (Panakova et al., 2005). However, co-expression of HA-Bou and ApoLII-Myc, the main protein component of lipophorin particles, revealed that these markers label different vesicle populations (Fig. 7I-K). Thus, HA-Bou extracellular transport is unlikely to rely on lipophorin particles.

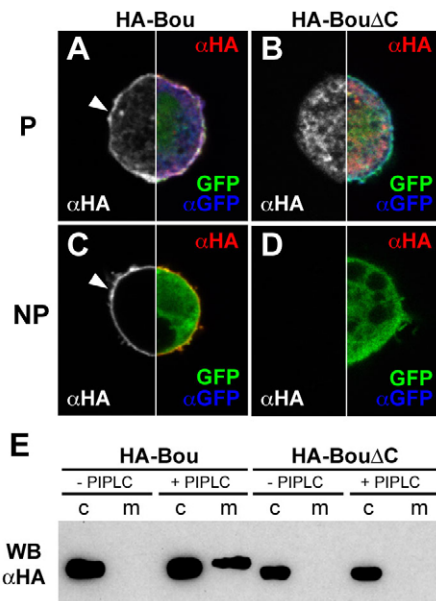


Fig. 5. Bou is a GPI-anchored membrane protein. (A–D) *Drosophila* S2 cells co-expressing Moesin-GFP (green, right panels) and HA-Bou (A, C) or HA-BouΔC (B, D). Staining with anti-HA (white, left panels; red, right panels) and anti-GFP (blue, right panels) was carried out in permeabilising (A, B) or non-permeabilising (C, D) conditions. White arrowheads indicate HA-Bou membrane accumulation. (E) Cellular fraction or culture medium of *Drosophila* Kc cells expressing HA-Bou or HA-BouΔC, blotted with anti-HA antibody. HA-Bou but not HA-BouΔC is released to the culture medium upon PI-PLC treatment. c, cellular fraction; m, culture medium.

***bou* function is required in a subset of neural tissues**

We show that *bou* function is essential for SJ assembly in epithelial tissues. However, SJs also play a physiological role in the glial cells forming the blood-brain barrier and isolating the insect neural tissues (Banerjee and Bhat, 2007). This prompted us to examine if *bou* is involved in the maintenance of this barrier in the embryonic chordotonal organs. These sensory mechanoreceptors are made of five units, each formed by three glial cells protecting a sensory bipolar neuron. Two of these glial cells, the cap cell and the scolopal cell, form a luminal cavity encapsulating the neuron cilial dendrite and forming SJs with each other to isolate this structure (Fig. 8A) (Carlson et al., 1997). The cell contacts between cap and scolopal cells accumulate SJ markers, such as NrX-IV and NrgGFP (Fig. 8B–F) (Banerjee et al., 2006). We performed dextran injections in stage-16 wild-type embryos and confirmed that this dye is excluded from the chordotonal lumen (Fig. 8B–D). By contrast, the dye diffused into this structure in *bou^{let}* embryos of the same stage (Fig. 8H–J), and the SJ markers appear delocalised (Fig. 8H–L). Therefore, *bou* is also required for SJ organisation in the chordotonal organs.

The embryonic ventral nerve cord is also protected by a specialised layer of glial cells, the subperineural glia, which form an efficient paracellular barrier (Schwabe et al., 2005; Stork et al., 2008). Performing dye injections in 22-hour-old embryos (Fig. 8M–O), we observed that this barrier was still functional in *bou^{let}* mutants, whereas, as expected, the dye penetrated into the nerve cord of *nrg¹⁴* mutants (Schwabe et al., 2005). Thus, the integrity of the central nervous system paracellular barrier does not depend on *bou* activity.

DISCUSSION

***bou* is required for SJ formation in different epithelial and neural tissues**

Our results reveal that Bou plays an essential role in the organisation of SJs and the maintenance of paracellular barriers in *Drosophila* epithelia and chordotonal organs. Although some vertebrate members of the Ly6 family are known to participate in cell-adhesion processes (Bamezai, 2004), this is the first example showing that they are required for the formation of this type of cellular junction. As *bou* is well conserved in other insect genomes, its role in SJ organisation could have been maintained during evolution. Invertebrate SJs and vertebrate tight junctions are considered analogous structures because both participate in the establishment of paracellular barriers, although they present a different organisation. However, vertebrates have adhesion structures functionally, morphologically and molecularly similar to insect pleated SJs (Bellen et al., 1998): the so-called paranodal septate junctions, which are formed by neural axons and Schwann cells, at the level of the Ranvier's nodes (Schafer and Rasband, 2006). We show that Bou is necessary for SJ organisation in the embryonic peripheral nervous system, indicating that its activity is required in some neural tissues. Thus, our observations raise the possibility that some vertebrate Ly6 proteins could be involved in the formation of paranodal septate junctions, which are essential for axonal insulation and propagation of action potentials.

In insects, the epithelial and neural SJs share many components, so our observation that *bou* is not required for blood-brain barrier maintenance in the ventral nerve cord came as a surprise, revealing the existence of tissular and molecular heterogeneities in the organisation of these junctions. It will be interesting to establish whether these differences also determine different barrier selective properties. We speculate that other Ly6 proteins expressed in the nervous system could contribute to blood-brain barrier formation in the subperineural glia.

A secreted factor participating in SJ assembly?

Our results show that *bou* inactivation specifically perturbs the organisation of SJs. As these structures are large extracellular complexes including different transmembrane and GPI-anchored proteins (Wu and Beitel, 2004), one hypothesis is that Bou could be a membrane SJ component. Consistently, HA-Bou is found at lateral contact areas in tracheal, salivary gland and wing disc epithelia, overlapping with the membrane domains that contain SJ. However, this protein does not significantly accumulate in these membrane regions and is also seen in the most apical part of the cells, opening up the possibility that it could operate in other membrane areas or act as a signalling molecule. Indeed, studies in vertebrates indicate that Ly6 proteins can assume roles in both cell signalling and cell adhesion (Bamezai, 2004). Clearly, identification of the Bou molecular partners will be a crucial step in understanding how this protein exerts its activity.

In contrast with other genes required for SJ formation (Genova and Fehon, 2003), *bou* functions in a non-cell-autonomous way. Accordingly, the Bou protein is found in extracellular particles and can be captured by neighbouring cells, suggesting that its diffusion is responsible for the phenotypic non-autonomy. Although it is possible that Bou could act as a secreted ligand after release of its GPI anchor, a parallelism with other members of the family suggests that the full molecule could instead become incorporated into the membrane of neighbouring cells (Neumann et al., 2007). In fact, the mammalian Ly6 member CD59, a cell-surface antigen protecting host cells from the complement attack, travels coupled to

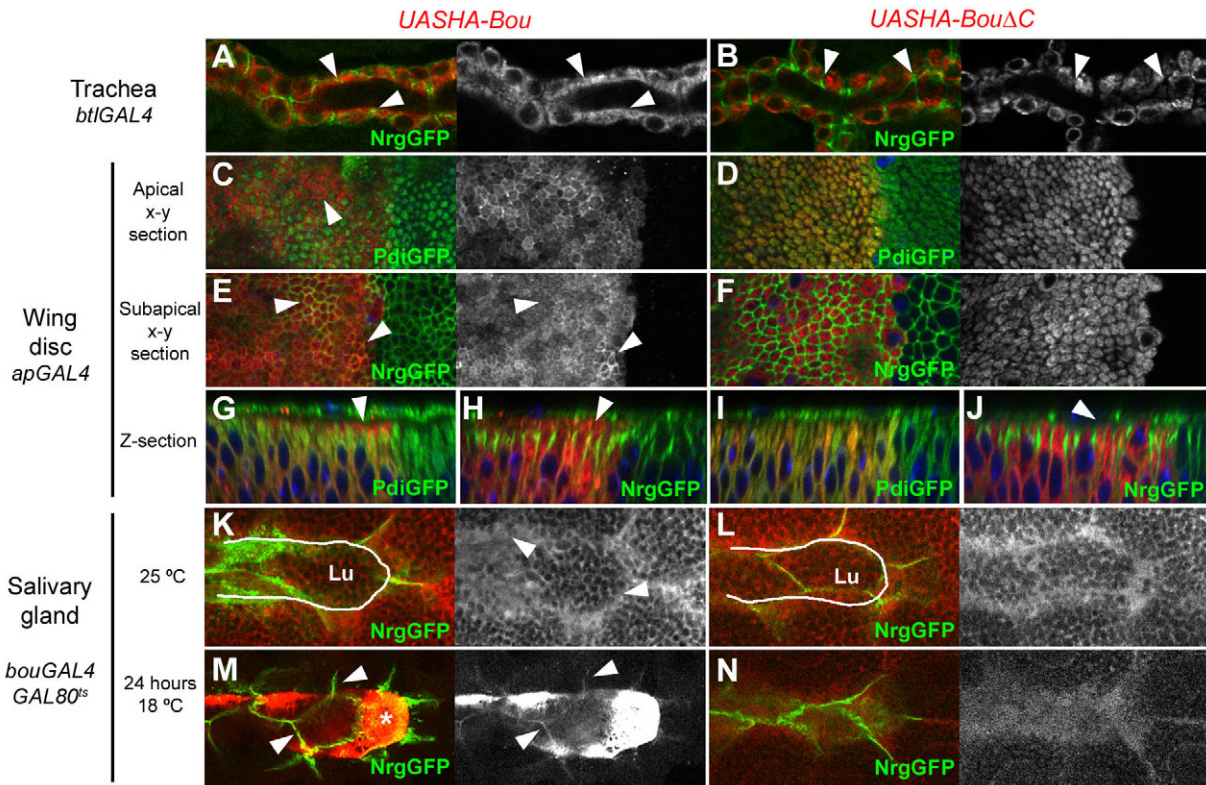


Fig. 6. HA-Bou is found in the membrane and is stabilised in SJ membrane areas. (A–J) Confocal sections showing HA-Bou and HA-Bou Δ C distribution (red) in tracheal cells (A,B) and wing discs (C–J) counterstained with NrgGFP or PdiGFP (green). HA-Bou overlaps with NrgGFP in membrane areas (A,E,H, arrowheads) and with PdiGFP in the cell body (C,G). HA-Bou Δ C colocalises with PdiGFP (D,I) but is excluded from membrane areas (B,F,J, arrowheads). (K–N) Single confocal sections featuring the luminal apical side of *bouGAL4/GAL80^{ts}* larval salivary gland cells expressing HA-Bou or HA-Bou Δ C. (K,L) At 25°C, both proteins stain the cell body. (M,N) Twenty-four hours after a shift to 18°C, the HA-Bou protein accumulates in the lumen surface (asterisk) and is seen colocalising with NrgGFP in lateral membrane regions (M, arrowheads), while HA-Bou Δ C levels decay uniformly (N). Lu, lumen.

membranous vesicles called prostasomes with its intact GPI. These specialised vesicles are secreted into the seminal fluid by prostatic glands, and allow CD59 transfer to the sperm cells, which can then elude complement attack (Rooney et al., 1993). GPI-bound CD59 has also been found associated with human HDL apolipoproteins (Vakeva et al., 1994). However, we show that the Bou particles are

not lipophorin vesicles, the insect equivalent to vertebrate apolipoproteins (Rodenburg and Van der Horst, 2005). Therefore, the fly wing epithelium could produce a different type of vesicle, possibly similar to prostasomes, which we propose to call ‘boudosomes’. Unfortunately, we could not determine whether the Bou GPI anchor is required for incorporation into these particles,

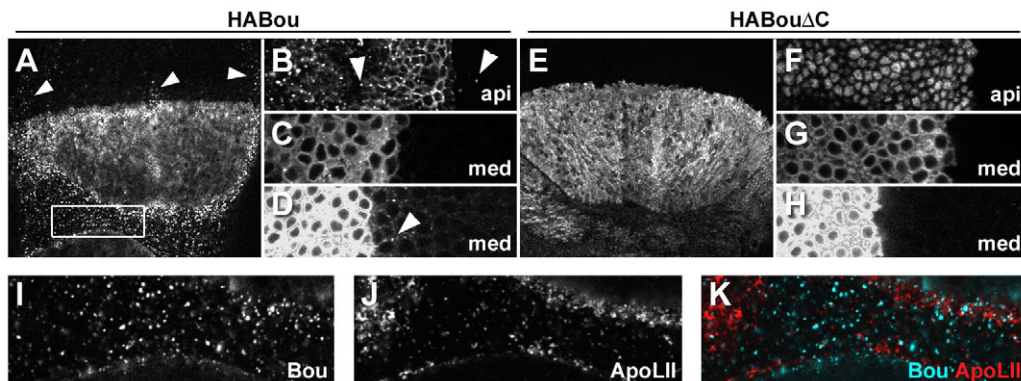


Fig. 7. The HA-Bou protein is present in extracellular particles. (A–H) Single confocal *x/y* sections of third-larval-instar wing discs stained with anti-HA antibody. HA-Bou accumulates apically in extracellular particles (A,B, arrowheads) and intracellular vesicles found in the medial regions of *apGAL4* cells (C) or contiguous cells (D, arrowhead). HA-Bou Δ C does not accumulate in any vesicular structure (E–H). (I–K) Higher magnification of framed area in A. HA-Bou (I, cyan in K) and ApoLII-Myc (J, red in K) label different populations of extracellular particles, as seen in merge channel (K). api, apical; med, medial.

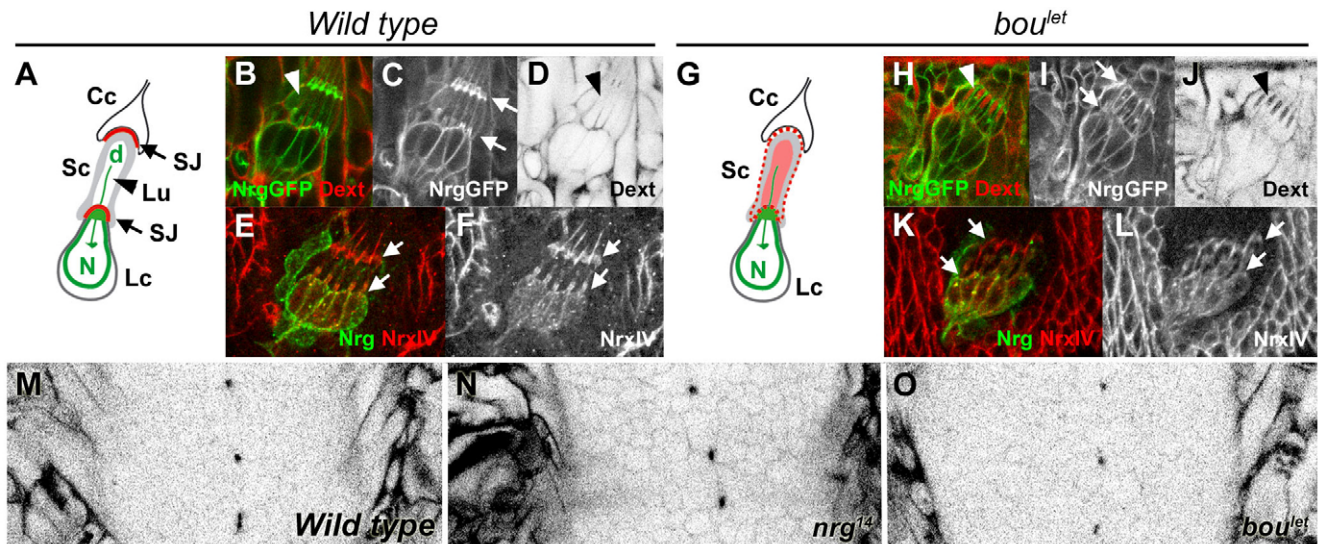


Fig. 8. The *bou* gene is required for blood-brain barrier maintenance in a subset of neural tissues. (A-L) Single confocal sections showing chordotonal organs of wild-type (A-F) and *bou^{let}* (G-L) stage-16 embryos. (A,G) Schematic representations of a single chordotonal organ unit. Injected dextran (red, B,H; black, D,J) diffuses into the lumen (arrowheads) of *bou^{let}* but not wild-type chordotonal organs. NrgGFP (green) and NrXIV (red) accumulate in wild-type SJ regions (B-F, arrows) but not in *bou^{let}* embryos (H-L). (M-O) Single confocal sections of ventral nerve cords of 22-hour live embryos injected with dextran (black). This dye fills intercellular spaces in *nrg¹⁴* but not wild-type or *bou^{let}* embryos. Cc, cap cell; d, dendrite; Lc, ligament cell; Lu, lumen; N, neuron; Sc, scolopal cell; SJ, SJ contacts.

because the C-terminus of the protein seems essential for prior exit from the ER. Thus, future work will be needed to characterise the biochemical features of bodosomes and their function.

Little is known about how epithelial cells coordinate their activity to form efficient fences. As many SJ components are required in a cell-autonomous manner (Genova and Fehon, 2003), their simultaneous expression by each individual cell seems a prerequisite for barrier assembly. A component and/or SJ regulator shared by different cells could be an element coordinating the organisation of efficient barriers in a dynamic epithelium. Alternatively, Bou extracellular traffic could be a specialised feature of this GPI-anchored protein and not have functional relevance for SJ assembly during normal development.

The *Drosophila* Ly6 family boom

Besides Bou and the TGF β receptors, the only member of the Ly6 fly family with a characterised role is the Rtv protein, which is also expressed in epidermal derivatives. We show that both *bou* and *rtv* mutants affect the organisation of the tracheal chitin luminal cable, although *rtv* mutants exhibit stronger phenotypes. However, SJ integrity is a prerequisite for proper assembly of the chitin cable (Swanson and Beitel, 2006), and we show that *rtv* is neither required for paracellular barrier integrity nor for SJ organisation. Thus, whereas our observations confirm that chitin cable deposition relies on the organisation of SJs, they demonstrate that these Ly6 proteins act in different processes.

We have carried out the first description of the Ly6 superfamily in the genome of an insect, identifying 36 new genes bearing this domain in *Drosophila*. The conservation of these proteins among the drosophilids indicates that the family was established before the evolutionary radiation of this group. By contrast, we have identified only 14 genes coding for Ly6 domains in the honeybee genome. Most of these genes have fly orthologues, like *bou* and *rtv*, pointing out the existence in higher insects of a core of ancestral genes with

potentially conserved roles. Thus, repeated events of gene duplication followed by rapid divergence of coding and regulatory sequences occurred in the drosophilid lineage. Indeed, the presence of genomic clusters grouping together different Ly6 genes is a novel evolutionary acquisition, as the conserved genes tend to be in isolated positions (Table 1).

It seems that genes coding for a Ly6 motif are prone to sudden phases of extensive duplication and diversification in different phylogenetic groups. In fact, an interesting parallelism can be drawn with the evolution of three-finger elapid snake venoms. This large group of Ly6 secreted proteins operates using diverse strategies, such as forming membrane pores, targeting the activity of acetylcholine receptors, inactivating acetylcholine esterase or blocking platelet aggregation (Tsetlin, 1999). Moreover, crystallographic analysis has revealed that three-finger toxins can interact with their targets via virtually any part of their solvent exposed surfaces (Kini, 2002). Yet, most of them share a common ancestor (Fry et al., 2003). Given the broad diversity of expression patterns exhibited by the different *Drosophila* Ly6 members, it is likely that gene duplication has been followed by acquisition of new developmental and physiological functions. Analysis of this insect family from an evolutionary perspective could be a way to enhance our understanding of the mechanisms underlying the generation of evolutionary innovations.

We are grateful to U. Tepass, H. Bellen, A. Debec, R. Martinho, H. Chanut, S. Eaton, L. García-Alles and F. Payre for kindly sharing antibodies, plasmids and mutant strains. We also thank the Bloomington Stock Center, the DRGC, the DSHB and the Toulouse RIO Imaging platform for making available fly stocks, reagents and imaging facilities. A.H. is recipient of a PhD fellowship awarded by the Lebanese CNRS. This work has been supported by grants from the ANR and the CNRS.

Supplementary material

Supplementary material for this article is available at <http://dev.biologists.org/cgi/content/full/136/13/2199/DC1>

References

- Altschul, S. F., Madden, T. L., Schaffer, A. A., Zhang, J., Zhang, Z., Miller, W. and Lipman, D. J.** (1997). Gapped BLAST and PSI-BLAST: a new generation of protein database search programs. *Nucleic Acids Res.* **25**, 3389-3402.
- Bamezai, A.** (2004). Mouse Ly-6 proteins and their extended family: markers of cell differentiation and regulators of cell signaling. *Arch. Immunol. Ther. Exp. (Warsz.)* **52**, 255-266.
- Banerjee, S. and Bhat, M. A.** (2007). Neuron-glia interactions in blood-brain barrier formation. *Annu. Rev. Neurosci.* **30**, 235-258.
- Banerjee, S., Pillai, A. M., Paik, R., Li, J. and Bhat, M. A.** (2006). Axonal ensheathment and septate junction formation in the peripheral nervous system of *Drosophila*. *J. Neurosci.* **26**, 3319-3329.
- Beitel, G. J. and Krasnow, M. A.** (2000). Genetic control of epithelial tube size in the *Drosophila* tracheal system. *Development* **127**, 3271-3282.
- Bellen, H. J., Lu, Y., Beckstead, R. and Bhat, M. A.** (1998). Neurexin IV, caspr and paranodin-novel members of the neurexin family: encounters of axons and glia. *Trends Neurosci.* **21**, 444-449.
- Blasi, F. and Carmeliet, P.** (2002). uPAR: a versatile signalling orchestrator. *Nat. Rev. Mol. Cell Biol.* **3**, 932-943.
- Bobinnec, Y., Marcaillou, C., Morin, X. and Debec, A.** (2003). Dynamics of the endoplasmic reticulum during early development of *Drosophila melanogaster*. *Cell Motil. Cytoskeleton* **54**, 217-225.
- Bourbon, H. M., Gonzy-Treboul, F., Peronnet, F., Alin, M. F., Ardourel, C., Benassayag, C., Cribbis, D., Deutsch, J., Ferrer, P., Haenlin, M. et al.** (2002). A P-insertion screen identifying novel X-linked essential genes in *Drosophila*. *Mech. Dev.* **110**, 71-83.
- Brand, A. H. and Perrimon, N.** (1993). Targeted gene expression as a means of altering cell fates and generating dominant phenotypes. *Development* **118**, 401-415.
- Carlson, S. D., Hilgers, S. L. and Juang, J. L.** (1997). Ultrastructure and blood-nerve barrier of chordotonal organs in the *Drosophila* embryo. *J. Neurocytol.* **26**, 377-388.
- Chimienti, F., Hogg, R. C., Plantard, L., Lehmann, C., Brakch, N., Fischer, J., Huber, M., Bertrand, D. and Hohl, D.** (2003). Identification of SLURP-1 as an epidermal neuromodulator explains the clinical phenotype of Mal de Meleda. *Hum. Mol. Genet.* **12**, 3017-3024.
- Coiffier, D., Charroux, B. and Kerridge, S.** (2008). Common functions of central and posterior Hox genes for the repression of head in the trunk of *Drosophila*. *Development* **135**, 291-300.
- Davies, A., Simmons, D. L., Hale, G., Harrison, R. A., Tighe, H., Lachmann, P. J. and Waldmann, H.** (1989). CD59, an LY-6-like protein expressed in human lymphoid cells, regulates the action of the complement membrane attack complex on homologous cells. *J. Exp. Med.* **170**, 637-654.
- Devine, W. P., Lubarsky, B., Shaw, K., Luschnig, S., Messina, L. and Krasnow, M. A.** (2005). Requirement for chitin biosynthesis in epithelial tube morphogenesis. *Proc. Natl. Acad. Sci. USA* **102**, 17014-17019.
- Dyson, H. J. and Wright, P. E.** (2002). Coupling of folding and binding for unstructured proteins. *Curr. Opin. Struct. Biol.* **12**, 54-60.
- Eisenhaber, B., Bork, P. and Eisenhaber, F.** (1998). Sequence properties of GPI-anchored proteins near the omega-site: constraints for the polypeptide binding site of the putative transamidase. *Protein Eng.* **11**, 1155-1161.
- Fry, B. G., Wuster, W., Kini, R. M., Brusich, V., Khan, A., Venkataraman, D. and Rooney, A. P.** (2003). Molecular evolution and phylogeny of elapid snake venom three-finger toxins. *J. Mol. Evol.* **57**, 110-129.
- Galat, A.** (2008). The three-fingered protein domain of the human genome. *Cell Mol. Life Sci.* **65**, 3481-3493.
- Genova, J. L. and Fehon, R. G.** (2003). Neuroglian, Gliotactin, and the Na⁺/K⁺ ATPase are essential for septate junction function in *Drosophila*. *J. Cell Biol.* **161**, 979-989.
- Grando, S. A.** (2008). Basic and clinical aspects of non-neuronal acetylcholine: biological and clinical significance of non-canonical ligands of epithelial nicotinic acetylcholine receptors. *J. Pharmacol. Sci.* **106**, 174-179.
- Huai, Q., Mazar, A. P., Kuo, A., Parry, G. C., Shaw, D. E., Callahan, J., Li, Y., Yuan, C., Bian, C., Chen, L. et al.** (2006). Structure of human urokinase plasminogen activator in complex with its receptor. *Science* **311**, 656-659.
- Kini, R. M.** (2002). Molecular moulds with multiple missions: functional sites in three-finger toxins. *Clin. Exp. Pharmacol. Physiol.* **29**, 815-822.
- Koh, K., Joiner, W. J., Wu, M. N., Yue, Z., Smith, C. J. and Sehgal, A.** (2008). Identification of SLEEPLESS, a sleep-promoting factor. *Science* **321**, 372-376.
- Lamb, R. S., Ward, R. E., Schweizer, L. and Fehon, R. G.** (1998). *Drosophila* coracle, a member of the protein 4.1 superfamily, has essential structural functions in the septate junctions and developmental functions in embryonic and adult epithelial cells. *Mol. Biol. Cell* **9**, 3505-3519.
- Lee, T., Winter, C., Marticke, S. S., Lee, A. and Luo, L.** (2000). Essential roles of *Drosophila* RhoA in the regulation of neuroblast proliferation and dendritic but not axonal morphogenesis. *Neuron* **25**, 307-316.
- Low, B. W., Preston, H. S., Sato, A., Rosen, L. S., Searl, J. E., Rudko, A. D. and Richardson, J. S.** (1976). Three dimensional structure of erabutoxin b neurotoxic protein: inhibitor of acetylcholine receptor. *Proc. Natl. Acad. Sci. USA* **73**, 2991-2994.
- McGuire, S. E., Le, P. T., Osborn, A. J., Matsumoto, K. and Davis, R. L.** (2003). Spatiotemporal rescue of memory dysfunction in *Drosophila*. *Science* **302**, 1765-1768.
- Miwa, J. M., Stevens, T. R., King, S. L., Caldaroni, B. J., Ibanez-Tallon, I., Xiao, C., Fitzsimonds, R. M., Pavlides, C., Lester, H. A., Picciotto, M. R. et al.** (2006). The protoxin lynx1 acts on nicotinic acetylcholine receptors to balance neuronal activity and survival *in vivo*. *Neuron* **51**, 587-600.
- Moussian, B., Soding, J., Schwarz, H. and Nusslein-Volhard, C.** (2005). Retroactive, a membrane-anchored extracellular protein related to vertebrate snake neurotoxin-like proteins, is required for cuticle organization in the larva of *Drosophila melanogaster*. *Dev. Dyn.* **233**, 1056-1063.
- Moussian, B., Tang, E., Tonning, A., Helms, S., Schwarz, H., Nusslein-Volhard, C. and Uv, A. E.** (2006). *Drosophila* Knickkopf and Retroactive are needed for epithelial tube growth and cuticle differentiation through their specific requirement for chitin filament organization. *Development* **133**, 163-171.
- Neumann, S., Harterink, M. and Sprong, H.** (2007). Hitch-hiking between cells on lipoprotein particles. *Traffic* **8**, 331-338.
- Oda, H., Uemura, T., Harada, Y., Iwai, Y. and Takeichi, M.** (1994). A *Drosophila* homolog of cadherin associated with armadillo and essential for embryonic cell-cell adhesion. *Dev. Biol.* **165**, 716-726.
- Panakova, D., Sprong, H., Marois, E., Thiele, C. and Eaton, S.** (2005). Lipoprotein particles are required for Hedgehog and Wingless signalling. *Nature* **435**, 58-65.
- Perrimon, N., Engstrom, L. and Mahowald, A. P.** (1989). Zygotic lethals with specific maternal effect phenotypes in *Drosophila melanogaster*. I. Loci on the X chromosome. *Genetics* **121**, 333-352.
- Ploug, M. and Ellis, V.** (1994). Structure-function relationships in the receptor for urokinase-type plasminogen activator. Comparison to other members of the Ly-6 family and snake venom alpha-neurotoxins. *FEBS Lett* **349**, 163-168.
- Pruitt, K. D., Tatusova, T. and Maglott, D. R.** (2007). NCBI reference sequences (RefSeq): a curated non-redundant sequence database of genomes, transcripts and proteins. *Nucleic Acids Res.* **35**, D61-D65.
- Rodenburg, K. W. and Van der Horst, D. J.** (2005). Lipoprotein-mediated lipid transport in insects: analogy to the mammalian lipid carrier system and novel concepts for the functioning of LDL receptor family members. *Biochim. Biophys. Acta* **1736**, 10-29.
- Rooney, I. A., Atkinson, J. P., Krul, E. S., Schonfeld, G., Polakoski, K., Saffitz, J. E. and Morgan, B. P.** (1993). Physiologic relevance of the membrane attack complex inhibitory protein CD59 in human seminal plasma: CD59 is present on extracellular organelles (prostasomes), binds cell membranes, and inhibits complement-mediated lysis. *J. Exp. Med.* **177**, 1409-1420.
- Schafer, D. P. and Rasband, M. N.** (2006). Glial regulation of the axonal membrane at nodes of Ranvier. *Curr. Opin. Neurobiol.* **16**, 508-514.
- Schwabe, T., Bainton, R. J., Fetter, R. D., Heberlein, U. and Gaul, U.** (2005). GPCR signaling is required for blood-brain barrier formation in *drosophila*. *Cell* **123**, 133-144.
- Stork, T., Engelen, D., Krudewig, A., Silies, M., Bainton, R. J. and Klambt, C.** (2008). Organization and function of the blood-brain barrier in *Drosophila*. *J. Neurosci.* **28**, 587-597.
- Swanson, L. E. and Beitel, G. J.** (2006). Tubulogenesis: an inside job. *Curr. Biol.* **16**, R51-R53.
- Tamura, K., Subramanian, S. and Kumar, S.** (2004). Temporal patterns of fruit fly (*Drosophila*) evolution revealed by mutation clocks. *Mol. Biol. Evol.* **21**, 36-44.
- Tepass, U. and Hartenstein, V.** (1994). The development of cellular junctions in the *Drosophila* embryo. *Dev. Biol.* **161**, 563-596.
- Tepass, U., Theres, C. and Knust, E.** (1990). crumbs encodes an EGF-like protein expressed on apical membranes of *Drosophila* epithelial cells and required for organization of epithelia. *Cell* **61**, 787-799.
- Tepass, U., Tanentzapf, G., Ward, R. and Fehon, R.** (2001). Epithelial cell polarity and cell junctions in *Drosophila*. *Annu. Rev. Genet.* **35**, 747-784.
- Tomancak, P., Beaton, A., Weiszmarm, R., Kwan, E., Shu, S., Lewis, S. E., Richards, S., Ashburner, M., Hartenstein, V., Celniker, S. E. et al.** (2002). Systematic determination of patterns of gene expression during *Drosophila* embryogenesis. *Genome Biol.* **3**, RESEARCH0088.
- Tonning, A., Hemphala, J., Tang, E., Nannmark, U., Samakovlis, C. and Uv, A.** (2005). A transient luminal chitinous matrix is required to model epithelial tube diameter in the *Drosophila* trachea. *Dev. Cell* **9**, 423-430.
- Tsetlin, V.** (1999). Snake venom alpha-neurotoxins and other 'three-finger' proteins. *Eur. J. Biochem.* **264**, 281-286.
- Vakeva, A., Jauhiainen, M., Ehnholm, C., Lehto, T. and Meri, S.** (1994). High-density lipoproteins can act as carriers of glycosphosphoinositol lipid-anchored CD59 in human plasma. *Immunology* **82**, 28-33.
- Waltzer, L., Ferjoux, G., Bataille, L. and Haenlin, M.** (2003). Cooperation between the GATA and RUNX factors Serpent and Lozenge during *Drosophila* hematopoiesis. *EMBO J.* **22**, 6516-6525.
- Wu, V. M. and Beitel, G. J.** (2004). A junctional problem of apical proportions: epithelial tube-size control by septate junctions in the *Drosophila* tracheal system. *Curr. Opin. Cell Biol.* **16**, 493-499.

Ly6/uPAR motifs of proteins containing a single domain (25 proteins)

	1	2	3	4	5
CG14430	CYV	CDTSDTEHPFQ	CGEWFERYDIPDIQPQN	CSSVHGAQF	CVKHVGRFEGGIGAKRF
CG1397	CYQ	CRSRGELGS	CKDPFTFNATDVEQEPGVAaip	CASGW	CGKVIIEGGGTYAIDDDYLAIQRM
CG2813	CYV	CNSQTGNTEK	CLNTIKT	CEPFENV	CGTEIRWGSQPYFSEGALKQYYVSKR
CG7781	CFV	CNSHKDAN	CALDIPPDNLLKD	CDEQYSSRGKGIPTY	CRKITQIIEFSVNSLPPDSRVIRT
CG14275	CHQ	CNSHDNED	CGGLVVNTPRAQRDNQYLTD	CVPPSGEVAF	CRKTVINFEQNDEERRIERS
CG14274	CYV	CSSDNPS	CADLGSNSSIVAAEE	CTLDKMKSLDTWLFDLNKFYSYFDNGANKSPLMN	CQKVVAKDPDTRKVVATARF
CG9568	CSK	CTSPSG	CKSPSSET	CNSTANANKEFLEGYHSNVPTVNGSLSFs	CANLTYHYHAANYTHTFEFLG
CG13102	CYT	CVTPKD	CKSPKKVT	CTNAAANETSYYLGVYHQVGNLTSTRFD	CLALKYNWNNDVIHQHLHG
CG6583	CYQ	CSSDQDRKGHDS	CGAYKRFNRTEHISIE	CNSDESHMPGSF	CMKVQQGPRGFIWDGRWRQVIRR
CG17218	CWD	CRSDNDPK	CGDPFDNSTLAITD	CQQAPELEHLKGVPTM	CRKIRQKVHGEWRYFRS
CG6579	CYQ	CKSLTDPN	CAKDKIDSASNIRAVD	CDSVPKPNTEQLQPVTR	CNKVVTSDRAGTIVSRD
CG15169	CYS	CMF	CNKTITNETKSN	CGPIPKRNG	CRTILLNDPNVVPKKYFLHRG
CG31676	CWR	CSTDVSNGEF	CNDPFMPETISEQQRYWSYVN	CTYSVGAKSVNARPV	CKKLVEVYGKRVISRS
CG31675	CYAC	ESVYEAS	CGDDFEVENHFKYD	CAFIAPPRFLENDLLSVNATA	CLKRVFKENGVRKIVRG
CG9335	CWH	CSSDTIGAEDF	CDVTFQEDNIPTDLIKERNINLLRS	CNGTINSHERAV	CRKTVEENNGKLITKRF
CG9336	CYQ	CESLTMPK	CGLKFEADETLLLD	CSRIGPPRYLQNFPLRNATG	CMKKTLESVAGHPQIVRS
CG9338	CYQ	CDSL TNSE	CGKDIKSDSSLVLD	CTKMAPP RFLQNF PVRNATG	CMKQTIDIPGNPQIVRS
CG14401	CYE	CDSVNGP	CGERFVGDDISTTD	CDVVANMRSLGAEAT	CLTKYHEGMPGDTRFVRRS
CG33472	CYE	CDSWTDAR	CKDPFNYTALPRDQPPLMT	CNGC	CVKMVRHQ RSPYEVVRRM
CG8501	CYE	VDQETS	CGSADNSPGRVRE	CPNSTM	CSTTMLTTMVGNEWIRVRRG
CG3955	CFAC	HTMDDGEA	CVDVAVRNDSALMKK	CQGEEFI	CMVKRFSYTTSTENSTSSPKMWSLDRR
CG6329	CYD	CNSEFDPR	CGDPFEPYSIGEVN	CSKQEPLEHLKDKYKPTL	CRKTVQKIYGKTRIVRG
CG6038	CYR	CTSATPG	CAEKFNWRGIGFLGEH	CPEPDDI	CVKVTERRGARETITRD
CG8861	CHM	CGQYNEGVGSITP	CTNYTTDIAHLYLKE	CTKKSEKF	CVKYVSELSTVRD
CG31323	CFK	CVSNGANKA	CDDPFHNNYSTAILESP	CMGGRKGRDGLFPATA	CIKIAGYYDGTGETITVRG

	6	7	8	9	10
CG14430	CSSKDMGNY	CDYVRNKGDRMDYRS	CIYT	CDTDG	CN
CG1397	CVQRGPDNDMDR	CADTIYNYKKVYM	CF	CQGD	CN
CG2813	CMTKEQ	CQSKRKRYMQLYCTHIWYEDWACNE	C	CKGDR	CN
CG7781	CAYQNQTSTNY	CYQRAGFGGRQVV	CS	CDTDN	CN
CG14275	CGFIPEKIQNA	CFTADNEGKQII	CT	CPDEG	CN
CG14274	CQLDTGDSDA	CEILRTKLRIPSPEEREQRNRNQNKRKRGHGQDAEEDDEISAEDAFF	CGI	CKSHR	CN
CG9568	CVFNETNV	CNLSLNNTASGWSK	CLQ	CGTDY	CN
CG13102	CVHPNVGA	CSLALKPAYAHYNKTW	CLT	CSGDK	CN
CG6583	CASVSDTGVVGV	CNWGVYENGVYWEE	CY	CSSDS	CN
CG17218	CAYMGEPGIEGDERF	CLMRTGSYNI FMEF	CT	CNSKDG	CN
CG6579	CHFESIGQKDNE	CTVTHSRQVES	CYT	CKGDL	CN
CG15169	CVSELDMELSRY	CAENEKL	CPT	CYEDN	CN
CG31676	CFYEDMDDSADK	CANDQTSSYIKTVY	CRT	CTTDG	CN
CG31675	CYFGEVNATDVW	CKMDPTLSAVQNSS	CHV	CDSENY	CN
CG9335	CYYTNKSDPVEL	CNITSPEKNVRRIF	CED	CLTDR	CN
CG9336	CYFGDINNIQAG	CQSDPSMPFVKQLG	CDV	CTKDE	CN
CG9338	CYFGNIADTKVG	CQTDPSLTINKLLS	CEV	CTEDE	CN
CG14401	CYFGDASPIGVS	CDDGPDVVPFMNFLG	CTL	CDTDL	CN
CG33472	CTSQLQINLFMVDHV	CMMESSGNHGM	CF	CEEDM	CN
CG8501	CAKQVDHYFDYIGKHWEQKYRLMDLPEG	CKKENGGRMN	CN	CRGEL	CN
CG3955	CTAN	CEPGCIIIGERTKLYSCTS	C	CEESF	CN
CG6329	CGYIPDENTDNK	CVRRSGTHDVAAIY	CS	CTKDL	CN
CG6038	CLSALSFRKDI PADKYEG	CRPAAHDEKLANYVNHTIKEHDVRRDY YTD TTF	CF	CFLDHR	CN
CG8861	CATE	CVEKEIWETQTY	C	CTEDG	CN
CG31323	CALDSGTLTTDTEIIRMSH	CGKFYYDDKYVHG	CLQS	CSDADA	CN

Disordered 10C domains (3 proteins)

	1	2	3	4		5	6	7	8	9	10			
CG14273	CYK	CED	--CDENTQLSEMEV	CESPLM	-----	118 residues	-----FCYTVRLQLNESTITKRG	CTTARRSNQTGG	CDGLFENWTVAG	-----	CQLCQDDG	CN		
CG7778	CYV	CDN	--CAQLPKDAPLLA	CNEDFFNPGGS	--	132 residues	--YTYHCYSVQVSVNGTMSTDRG	CSRVTMEGV	--CEQLKIQNKNTELAN	--	CNPCSMNACA			
CG31901	CYS	CVGNE	CHVETVPTVT	--CTLDDV	-----	426 residues	-YKIAACYSIYKDGEINRG	----	CVKVPEKHSG	--	CQAVRNELGITEDSADQ	CDCI	CLTNL	CN

Atypical 10C domains (2 proteins)

	1	2	3	4	5	6	7	8	9	10				
CG15773 1	CLQ	CTHNRLAPNPD	CLRDQDPPAAVAEDQPK	CSSLNSTVTH	CVNKVMYGHREN	--	CFSYRNTQTEVLQRG	CSTAMGFYPTGELTE	---	CHGEF	-CNADC			
CG15170 3	CAT	CDSAIGRG	---	CKIDLFQVNTGR	-----	CNVSLYEE	--	CQQDVLLGEQEDKY	CFSFRRLSRVVRG	--	CSTKIPTDLEPYVEQLEK	CNTSDH	CNAGC	

8C domains (2 proteins)

	1	2	3	4	5	6	7	8					
CG15170 1	CYH	CDSIALPE	CSQTLGEVGVLPYKE	CATELT	-----	CAMSIVDSITYRG	--	CGAETPIGATYSKT	-----	CSTNL	CN		
CG15170 2	CHH	CAGQE	---	CVAAPASKPKP	----	CRYHLEEDQ	---	CYTDVISSSDAYRG	-	CTSEQNHTLSTSAQL	-----	CEING	CN
CG13492 3	CNV	CKGD	---	CSNPQSKT	-----	CRAVPSGDKPES	CFIEFDESGAIYEMG	CLSQYNVSDVTLLETNKQLWY	CTGDN	CN			
CG13492 7	CYK	CSGSD	---	CDDPKASQ	-----	CSQYSPDDR	---	CYILFDYNADITGMG	CLSDLDEEYVDENFHSLLF	--	CDDND	CN	
CG13492 12	CNV	CEDDA	---	CETLTSQL	-----	CLGYRSGDQ	---	CYIHVGDLISIKAMG	-	CATDLQDSFLLTNRDLYL	--	CSGDD	CN
CG13492 17	CYT	CKDPF	---	CEDPTTSK	-----	CVAYRENDQ	---	CYLAYDDSGVVAMG	-	CASEFEVQVIKELVAQQRLLL	CSGQK	CN	
CG13492 22	CLV	CQGDE	---	CQSPQASS	-----	CSNYREHDE	---	CYIQFDEERSITSLG	CLSELSHDDIYLLKRSKRLLT	CSDND	CN		
CG13492 27	CYT	CEGDD	---	CEDPQPKT	-----	CTIYKPEDS	---	CFLWVEDNDLKQLG	CLSSFRNQDLEAI	IKTKRISV	CNGT	CN	
CG13492 32	CHT	CLDDT	---	CSSSQSQA	-----	CLAYKTNDY	---	CFAKYATDGKVELMG	CASSQNESSLEQWQEGNLLYS	CQGSE	CN		

Ectodomains of TGFβ receptors type I (3 proteins) and II (2 proteins)

Type I receptors

	1	2	3	4	5	6	7	8	9	10						
Babo	CH	-	CDT	-	CKESNNI	---	CETDGF	--	CFTSVEKNSDGSII	FSYR	-----	CLHKSQIFPPGRSIW	CNDGLHGGPTARPVGRNGAHA	--	CCKDRDF	CN
Tkv	CY	-	CDGS	CPDNVSNGT	-	CETRPGGS	CFSAVQQLYDETTGMYEEERTYG	-	CMPPEDNGGFLM	---	CKVAAVPHLHGKNIV	-----	CCDKEDF	CN		
Sax	CYS	CEPP	CRDPYEFTH	CTQNAIQ	--	CWKSRTDADGQVQESRG	-----	CSTSPDQLPMI	----	CSQNSLKINGPSKRNTGKFVNVV	CCAGDY	-	CN			

Type II receptors

	1	2	3	4	5	6	7	8	9	10					
Punt	CEHFDEKM	CNTTQQ	CETRIEH	-----	CKMEADKFPS	CYVLWSVNETTGILRIKMKG	CFTDMHE	----	CNQTECVTSAEPRQGN	IHF	-	CCC	KGS	R	CN
Wit	CMSYQEDD	NSFHDDDDGDQDSSGELQE	QVESTPIPSEPHRRT	CPDGYTF	---	CF	TIWNQTANGARVVKQG	--	CWKDNTDRTSI	CSQSE	CTSSAPTSKTS	SSLY	CCC	SGGV	CN

Wild type

bou^{let}

